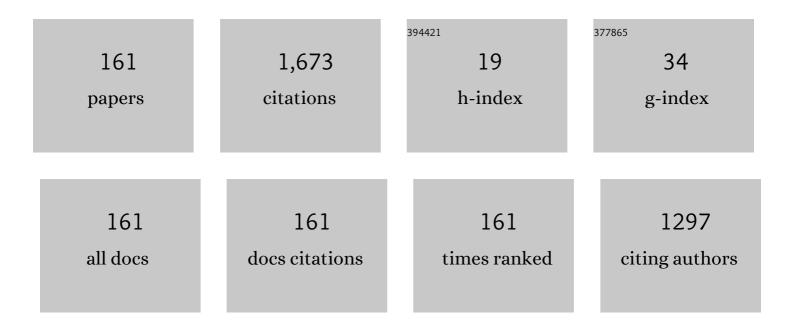
Dmitriy Yu Kovalev

List of Publications by Year in descending order

Source: https://exaly.com/author-pdf/6360391/publications.pdf Version: 2024-02-01



#	Article	IF	CITATIONS
1	On the mechanism of heterogeneous reaction and phase formation in Ti/Al multilayer nanofilms. Acta Materialia, 2005, 53, 1225-1231.	7.9	114
2	Dynamics of phase transformation during thermal explosion in the Al–Ni system: Influence of mechanical activation. Physica B: Condensed Matter, 2010, 405, 778-784.	2.7	91
3	Influence of the high energy ball milling on structure and reactivity of the Ni+Al powder mixture. Journal of Alloys and Compounds, 2013, 577, 600-605.	5.5	75
4	New Insight into the Formation of Hybrid Perovskite Nanowires via Structure Directing Adducts. Chemistry of Materials, 2017, 29, 587-594.	6.7	68
5	In Situ Preparation of Highly Stable Ni-Based Supported Catalysts by Solution Combustion Synthesis. Journal of Physical Chemistry C, 2014, 118, 26191-26198.	3.1	58
6	Anomalous Hall effect in granular Fe/SiO2 films in the tunneling-conduction regime. JETP Letters, 1999, 70, 90-96.	1.4	51
7	Self-propagating high-temperature synthesis of advanced ceramics in the Mo–Si–B system: Kinetics and mechanism of combustion and structure formation. Ceramics International, 2014, 40, 6541-6552.	4.8	51
8	Self-propagating high-temperature synthesis of advanced ceramics MoSi2–HfB2–MoB. Ceramics International, 2019, 45, 96-107.	4.8	43
9	Structure and properties of equiatomic CoCrFeNiMn alloy fabricated by high-energy ball milling and spark plasma sintering. Journal of Alloys and Compounds, 2019, 805, 1237-1245.	5.5	41
10	Production of ultra-high temperature carbide (Ta,Zr)C by self-propagating high-temperature synthesis of mechanically activated mixtures. Ceramics International, 2015, 41, 8885-8893.	4.8	39
11	Self-propagating high-temperature synthesis of nanocomposite ceramics TaSi2-SiC with hierarchical structure and superior properties. Journal of the European Ceramic Society, 2018, 38, 433-443.	5.7	36
12	Combustion synthesis of TiC-based ceramic-metal composites with high entropy alloy binder. Journal of the European Ceramic Society, 2020, 40, 2527-2532.	5.7	35
13	Crystallization of amorphous Cu50Ti50 alloy prepared by high-energy ball milling. Journal of Alloys and Compounds, 2018, 741, 575-579.	5.5	32
14	Solution combustion synthesis of nano-catalysts with a hierarchical structure. Journal of Catalysis, 2018, 364, 112-124.	6.2	29
15	Structural evolution and magnetic properties of high-entropy CuCrFeTiNi alloys prepared by high-energy ball milling and spark plasma sintering. Journal of Alloys and Compounds, 2020, 816, 152611.	5.5	29
16	Effect of mechanical activation on thermal explosion in Ni-Al mixtures. International Journal of Self-Propagating High-Temperature Synthesis, 2010, 19, 120-125.	0.5	27
17	Combustion synthesis of high-temperature ZrB2-SiC ceramics. Journal of the European Ceramic Society, 2018, 38, 2792-2801.	5.7	26
18	Exothermic Self-Sustained Waves with Amorphous Nickel. Journal of Physical Chemistry C, 2016, 120, 5827-5838.	3.1	23

#	Article	IF	CITATIONS
19	Combustion synthesis of ZrB2-TaB2-TaSi2 ceramics with microgradient grain structure and improved mechanical properties. Ceramics International, 2019, 45, 1503-1512.	4.8	22
20	Formation of nanolaminate structures in the Ti-Si-C system: A crystallochemical study. International Journal of Self-Propagating High-Temperature Synthesis, 2014, 23, 217-221.	0.5	20
21	Fabrication of high-entropy carbide (TiZrHfTaNb)Ð; by high-energy ball milling. Ceramics International, 2021, 47, 32626-32633.	4.8	20
22	Self-propagating high-temperature synthesis in the Ti-Si-C system: Features of product patterning. Nanotechnologies in Russia, 2015, 10, 67-74.	0.7	19
23	The kinetics and mechanism of combusted Zr–B–Si mixtures and the structural features of ceramics based on zirconium boride and silicide. Ceramics International, 2016, 42, 16758-16765.	4.8	18
24	One-step synthesis of pure γ-FeNi alloy by reaÑŧive sol–gel combustion route: mechanism and properties. Journal of Sol-Gel Science and Technology, 2020, 94, 310-321.	2.4	18
25	Combustion of Ti–Al–C compacts in air and helium: A TRXRD study. International Journal of Self-Propagating High-Temperature Synthesis, 2016, 25, 30-34.	0.5	17
26	Single crystals of ferroelectric lithium niobate–tantalate LiNb _{1–<i>x</i>} Ta <i> _{ <i>x</i>} </i> O ₃ solid solutions for high-temperature sensor and actuator applications. Acta Crystallographica Section B: Structural Science, Crystal Engineering and Materials, 2020, 76, 1071-1076.	1.1	17
27	Equilibrium of Products of Self-Propagating High-Temperature Synthesis. Doklady Physical Chemistry, 2004, 394, 34-38.	0.9	16
28	Thermal decomposition of TiH2: A TRXRD study. International Journal of Self-Propagating High-Temperature Synthesis, 2010, 19, 253-257.	0.5	16
29	The features of combustion and structure formation of ceramic materials in the TiC–Ti3POx–CaO system. Ceramics International, 2015, 41, 8177-8185.	4.8	16
30	Structure and properties of MoSi2–MeB2–SiC (Me = Zr, Hf) ceramics produced by combination of SHS and HP techniques. Ceramics International, 2020, 46, 28725-28734.	4.8	16
31	Fast mechanical synthesis, structure evolution, and thermal stability of nanostructured CoCrFeNiCu high entropy alloy. Journal of Alloys and Compounds, 2022, 893, 161839.	5.5	16
32	Evolution of crystal structure in high-entropy AlCoCrFeNi alloy: An in situ high-temperature X-ray diffraction study. Journal of Alloys and Compounds, 2021, 861, 158562.	5.5	15
33	Criteria of the Critical State of the Ni—Al System during Mechanical Activation. Combustion, Explosion and Shock Waves, 2010, 46, 457-463.	0.8	14
34	Silicon carbide ceramics SHS-produced from mechanoactivated Si–C–B mixtures. International Journal of Self-Propagating High-Temperature Synthesis, 2015, 24, 119-127.	0.5	14
35	Phase formation dynamics upon thermal explosion synthesis of magnesium diboride. Ceramics International, 2016, 42, 2951-2959.	4.8	14
36	Reaction synthesis of the Ti2AlN MAX-phase. Russian Journal of Non-Ferrous Metals, 2017, 58, 303-307.	0.6	14

3

#	Article	IF	CITATIONS
37	High-temperature synthesis of cast materials based on Nb2AlC MAX phase. Ceramics International, 2019, 45, 2689-2691.	4.8	14
38	Autowave Propagation of Exothermic Reactions in Ti–Al Thin Multilayer Films. Doklady Physical Chemistry, 2001, 381, 283-287.	0.9	13
39	Structural features and magnetic behavior of nanocrystalline powders of terbium oxide prepared by the thermal decomposition of terbium acetate in air. Journal of Alloys and Compounds, 2016, 657, 163-173.	5.5	13
40	Time-Resolved X-Ray Diffraction in SHS Research and Related Areas: An Overview. International Journal of Self-Propagating High-Temperature Synthesis, 2019, 28, 114-123.	0.5	13
41	Synthesis, Structure and Properties of Material Based on V2AlC MAX Phase. Physics of Metals and Metallography, 2020, 121, 765-771.	1.0	13
42	Assembling the Puzzle of Taxifolin Polymorphism. Molecules, 2020, 25, 5437.	3.8	12
43	Solution combustion synthesis: Dynamics of phase formation for highly porous nickel. Doklady Physical Chemistry, 2013, 449, 48-51.	0.9	11
44	SHS of MAX compounds in the Ti-Si-C system: Influence of mechanical activation. International Journal of Self-Propagating High-Temperature Synthesis, 2014, 23, 141-144.	0.5	11
45	High-Energy Ball Milling and Spark Plasma Sintering of the CoCrFeNiAl High-Entropy Alloy. Metals, 2020, 10, 1489.	2.3	11
46	The Concentration of C(sp3) Atoms and Properties of an Activated Carbon with over 3000 m2/g BET Surface Area. Nanomaterials, 2021, 11, 1324.	4.1	11
47	The features of combustion and structure formation of ceramic materials in the Cr–Al–Si–B system. Ceramics International, 2014, 40, 16299-16308.	4.8	10
48	Self-sustained exothermal waves in amorphous and nanocrystalline films: A comparative study. Journal of Alloys and Compounds, 2018, 749, 44-51.	5.5	10
49	Engineering of strong and hard in-situ Al-Al3Ti nanocomposite via high-energy ball milling and spark plasma sintering. Journal of Alloys and Compounds, 2022, 895, 162676.	5.5	10
50	Flameless Combustion Synthesis of Ni and Ag Nanoparticles in Ballasted Systems: A Timeâ€Resolved Xâ€ray Diffraction Study. Propellants, Explosives, Pyrotechnics, 2015, 40, 88-94.	1.6	9
51	Determination of the Thermal Expansion Coefficient of Boron Carbide Đ'13Đ¡2. High Temperature, 2018, 56, 668-672.	1.0	9
52	Thermal Expansion of Micro- and Nanocrystalline HfB2. High Temperature, 2019, 57, 32-36.	1.0	9
53	Self-Propagating High-Temperature Synthesis of MgAl2O4 Spinel. Inorganic Materials, 2020, 56, 142-150.	0.8	9
54	Phase Formation in the SHS of a Ti–B Mixture with the Addition of Si3N4. Combustion, Explosion and Shock Waves, 2020, 56, 648-654.	0.8	9

#	Article	IF	CITATIONS
55	Regular features of combustion of CaO2/Al/Ti/Cr/B hybrid mixtures. Combustion, Explosion and Shock Waves, 2011, 47, 671-676.	0.8	8
56	SHS hydrogenation of titanium: Some structural and kinetic features. International Journal of Self-Propagating High-Temperature Synthesis, 2013, 22, 114-118.	0.5	8
57	Synthesis of the Ti2AlC MAX Phase with a Reduction Step via Combustion of a TiO2 + Mg + Al + C Mixture. Inorganic Materials, 2018, 54, 949-952.	0.8	8
58	Phase Formation in the Ti–Al–C System during SHS. Russian Journal of Non-Ferrous Metals, 2019, 60, 61-67.	0.6	8
59	Mechanical alloying in the Co-Fe-Ni powder mixture: Experimental study and molecular dynamics simulation. Powder Technology, 2022, 399, 117187.	4.2	8
60	Dynamics of phase formation during combustion of Zr and Hf in air. International Journal of Self-Propagating High-Temperature Synthesis, 2007, 16, 169-174.	0.5	7
61	Behavior of the Ti-Al system during mechanical activation. International Journal of Self-Propagating High-Temperature Synthesis, 2013, 22, 56-59.	0.5	7
62	Synthesis of a new MAX phase in the Ti–Zr–Al–C system. Mendeleev Communications, 2017, 27, 59-60.	1.6	7
63	Processing of Ni–Al intermetallic with 2D carbon components. Materials Chemistry and Physics, 2019, 238, 121898.	4.0	7
64	Synthesis of Nb2AlC MAX Phase by SHS Metallurgy. Russian Journal of Non-Ferrous Metals, 2020, 61, 126-131.	0.6	7
65	Thermal Stability of Medium- and High-Entropy Alloys of 3d-Transition Metals. Journal of Phase Equilibria and Diffusion, 2021, 42, 720-734.	1.4	7
66	Comprehensive Study on the Mechanism of Sulfating Roasting of Zinc Plant Residue with Iron Sulfates. Materials, 2021, 14, 5020.	2.9	7
67	X-ray diffraction study of self-propagating high-temperature synthesis in the Zr–Al–C system. Russian Journal of Inorganic Chemistry, 2017, 62, 1638-1644.	1.3	7
68	Combustion of a Fe2O3-TiO2-Al-C Powder Mixture in the SHS Regime and the Structure of the Combustion Products. Combustion, Explosion and Shock Waves, 2005, 41, 414-420.	0.8	6
69	Cast silicides of molybdenum, tungsten, and niobium by combustion synthesis. International Journal of Self-Propagating High-Temperature Synthesis, 2011, 20, 100-106.	0.5	6
70	SHS of TiC-TiNi composites: Effect of initial temperature and nanosized refractory additives. International Journal of Self-Propagating High-Temperature Synthesis, 2012, 21, 202-211.	0.5	6
71	SHS in the Ni-Al system: A TRXRD study of product patterning. International Journal of Self-Propagating High-Temperature Synthesis, 2014, 23, 101-105.	0.5	6
72	Preparation of Ti2AlN by reactive sintering. International Journal of Self-Propagating High-Temperature Synthesis, 2016, 25, 35-38.	0.5	6

#	Article	IF	CITATIONS
73	Time-resolved X-ray diffraction study of the transition of an amorphous TiCu alloy to the crystalline state. Doklady Physics, 2017, 62, 111-114.	0.7	6
74	Transformations of Iron (III) Precursors in a Wave of Flameless RDX Combustion. International Journal of Self-Propagating High-Temperature Synthesis, 2018, 27, 162-166.	0.5	6
75	Effects of titanium high energy ball milling on the solid-phase reaction Ti+C. Materials Chemistry and Physics, 2022, 283, 126025.	4.0	6
76	SHS of boron carbide: Influence of combustion temperature. International Journal of Self-Propagating High-Temperature Synthesis, 2015, 24, 33-37.	0.5	5
77	Combustion synthesis in the Ni–Al–Nb ternary system: A Time-Resolved X-ray Diffraction study. Results in Physics, 2017, 7, 1878-1882.	4.1	5
78	lgnition and phase formation in the Zr–Al–C system. Combustion, Explosion and Shock Waves, 2017, 53, 171-175.	0.8	5
79	The features of combustion synthesis of aluminum and carbon doped magnesium diboride. Physica C: Superconductivity and Its Applications, 2017, 541, 1-9.	1.2	5
80	Thermal expansion of the nanocrystalline titanium diboride. Ceramics International, 2022, 48, 872-878.	4.8	5
81	Combustion synthesis in the Ni-Al-W system: Some structural features. International Journal of Self-Propagating High-Temperature Synthesis, 2013, 22, 110-113.	0.5	4
82	Mechanochemical Synthesis of Dy2TiO5 Single-Phase Crystalline Nanopowders and Investigation of Their Properties. Inorganic Materials: Applied Research, 2018, 9, 291-296.	0.5	4
83	High-Temperature X-ray Diffraction Study of the Thermal Expansion and Stability of Nanocrystalline VB2. Inorganic Materials, 2019, 55, 1111-1117.	0.8	4
84	Synthesis of Vanadium Diboride Nanoparticles via Reaction of VCl3 with NaBH4. Inorganic Materials, 2020, 56, 126-131.	0.8	4
85	Estimation of Enthalpy of Formation of TiCu by Density Functional Method. Physics of Metals and Metallography, 2020, 121, 1188-1192.	1.0	4
86	FEATURES OF PRODUCTION AND HIGH-TEMPERATURE OXIDATION OF SHS-CERAMICS BASED ON ZIRCONIUM BORIDE AND ZIRCONIUM SILICIDE. Izvestiya Vuzov Poroshkovaya Metallurgiya I Funktsional'nye Pokrytiya, 2017, , 29-41.	0.2	4
87	Synthesis and Thermal Oxidation Stability of Nanocrystalline Niobium Diboride. Inorganic Materials, 2021, 57, 1005-1014.	0.8	4
88	The mechanism of formation of copper aluminide in the thermal explosion mode. Russian Chemical Bulletin, 2000, 49, 1954-1959.	1.5	3
89	Phase constitution of the combustion products of thermite mixtures modified by titanium oxide. Combustion, Explosion and Shock Waves, 2007, 43, 674-681.	0.8	3
90	Effect of heat release conditions on the phase composition of the combustion products of a Fe2O3/TiO2/Al/C thermite mixture. Combustion, Explosion and Shock Waves, 2008, 44, 405-409.	0.8	3

#	Article	IF	CITATIONS
91	SHS of graded Ti-Al-C ceramics: Composition of transition layers. International Journal of Self-Propagating High-Temperature Synthesis, 2012, 21, 231-235.	0.5	3
92	Deposition of Ni-Al coatings onto copper by mechanical/heat treatment. International Journal of Self-Propagating High-Temperature Synthesis, 2013, 22, 103-109.	0.5	3
93	SHS hydrogenation of group IV metals as studied by time-resolved XRD. International Journal of Self-Propagating High-Temperature Synthesis, 2014, 23, 198-202.	0.5	3
94	Formation of nanosized particles of nickel and silver in a wave of flameless combustion of cellulose nitrate in ballasted systems. Doklady Physical Chemistry, 2014, 458, 133-137.	0.9	3
95	Mechanical activation of a hard magnetic Fe-Cr-Co alloy powder charge. Russian Metallurgy (Metally), 2014, 2014, 555-560.	0.5	3
96	Magnesiothermic SHS of boron carbide in conditions of temperature gradients. International Journal of Self-Propagating High-Temperature Synthesis, 2015, 24, 216-219.	0.5	3
97	SHS in the Zr–Al–C system: A time-resolved XRD study. International Journal of Self-Propagating High-Temperature Synthesis, 2016, 25, 149-154.	0.5	3
98	Dynamics of phase formation during the synthesis of magnesium diboride from elements in thermal explosion mode. Russian Journal of Non-Ferrous Metals, 2017, 58, 396-404.	0.6	3
99	Metal-Doped MgB2 by Thermal Explosion: A TRXRD Study. International Journal of Self-Propagating High-Temperature Synthesis, 2018, 27, 18-25.	0.5	3
100	Synthesis of Zirconium Diboride Nanoparticles by the Reaction of ZrCl4 with NaBH4 in an Ionic Potassium Bromide Melt. Russian Journal of General Chemistry, 2018, 88, 1757-1758.	0.8	3
101	Features of Production and High-Temperature Oxidation of SHS Ceramics Based on Zirconium Boride and Zirconium Silicide. Russian Journal of Non-Ferrous Metals, 2018, 59, 311-322.	0.6	3
102	Feasibility of Producing a Ti–Zr Alloy via Combustion in the TiO2–ZrO2–Mg System. Inorganic Materials, 2019, 55, 185-190.	0.8	3
103	Thermal Expansion of Micro- and Nanocrystalline ZrB2 Powders. Inorganic Materials, 2020, 56, 258-264.	0.8	3
104	Formation of new intermetallic phases in the Ta – Ni – Al system. Perspektivnye Materialy, 2019, , 5-13.	0.1	3
105	Title is missing!. Combustion, Explosion and Shock Waves, 2001, 37, 673-677.	0.8	2
106	Crystallization of a Mechanically Activated CuTi Alloy. Doklady Physics, 2018, 63, 45-49.	0.7	2
107	Conductive TiB2–AlN–BN-Based Composite SHS Ceramics. Russian Journal of Non-Ferrous Metals, 2018, 59, 658-663.	0.6	2
108	Crystallization of Amorphous Antimony at Room Temperature: Non-Uniqueness of Patterning Route. International Journal of Self-Propagating High-Temperature Synthesis, 2018, 27, 180-183.	0.5	2

#	Article	IF	CITATIONS
109	Composition and Structure of (Zr0.37Ti0.63)3AlC2 MAX Phase Crystals Prepared by Self-Propagating High-Temperature Synthesis. Inorganic Materials, 2018, 54, 953-956.	0.8	2
110	TiZrNiCuAl and TiNbNiCuAl Alloys by Thermal Explosion and High-Energy Ball Milling. International Journal of Self-Propagating High-Temperature Synthesis, 2019, 28, 137-142.	0.5	2
111	Preparation of ZrB2 by Reacting ZrCl4 with NaBH4 in Molten Potassium Bromide. Inorganic Materials, 2019, 55, 458-461.	0.8	2
112	Boron Carbide Secrets. Russian Journal of General Chemistry, 2019, 89, 2069-2074.	0.8	2
113	Synthesis, Structure, and Properties of Titanium Diboride Nanoparticles. Inorganic Materials, 2020, 56, 1127-1132.	0.8	2
114	High temperature X-ray powder diffraction study of boron carbide crystals of different composition. Journal of Solid State Chemistry, 2020, 290, 121579.	2.9	2
115	Synthesis of the Ti3SiC2 MAX Phase via Combustion in the TiO2–Mg–Si–C System. Inorganic Materials, 2020, 56, 1211-1216.	0.8	2
116	Preparation of Ti2AlC and Ti3AlC2 MAX Phases by Self-Propagating High-Temperature Synthesis with the Reduction Stage. Russian Journal of Non-Ferrous Metals, 2020, 61, 554-558.	0.6	2
117	DFT – Driven design of hierarchically structured, strong and highly conductive alloys in Cu–Ti system via in situ hydration - re-oxidation. Journal of Alloys and Compounds, 2020, 832, 154823.	5.5	2
118	Synthesis of Titanium Diboride Nanoparticles via the Reaction of TiCl4 with NaBH4 in NaCl‒KCl Ionic Melt. Russian Journal of General Chemistry, 2020, 90, 924-926.	0.8	2
119	Spall Strength of Shock-Heated Zirconium and Phase Diagram of Its High-Pressure Polymorphic Modification. Physics of the Solid State, 2020, 62, 65-73.	0.6	2
120	PHASE FORMATION IN TI–AL–C SYSTEM DURING SHS. Izvestiya Vuzov Poroshkovaya Metallurgiya I Funktsional'nye Pokrytiya, 2017, , 11-18.	0.2	2
121	Nb2AIC MAX phase synthesis by SHS metallurgy. Izvestiya Vuzov Poroshkovaya Metallurgiya I Funktsional'nye Pokrytiya, 2019, , 42-48.	0.2	2
122	Cu-Matrix Composites by Reactive Spark Plasma Sintering of Mechanoactivated Cu–Si–C Powder Mixtures. International Journal of Self-Propagating High-Temperature Synthesis, 2020, 29, 233-236.	0.5	2
123	High-Temperature Synthesis of Cr–Mo–Al–C Materials. Inorganic Materials, 2021, 57, 1300-1306.	0.8	2
124	2-dimensional GEM detector with FEE based on the nXYTER ASIC. Journal of Instrumentation, 2014, 9, C09026-C09026.	1.2	1
125	Experimental investigation of electrical and optical phenomena during combustion of two-layer energetic condensed (Zr + CuO + LiF)–(Zr + BaCrO4 + LiF) systems. Inorganic Materials: Applied Research, 2015, 6, 542-546.	0.5	1
126	Influence of synthesis conditions on the structure and phase formation during the SHS hydration of titanium. Russian Journal of Non-Ferrous Metals, 2015, 56, 86-91.	0.6	1

#	Article	IF	CITATIONS
127	Oxynitrides by aluminothermic SHS in nitrogen gas: Influence of nitrogen pressure. International Journal of Self-Propagating High-Temperature Synthesis, 2017, 26, 71-74.	0.5	1
128	Density Functional Calculations for Disordered Boron Carbide Crystals. Russian Journal of Physical Chemistry A, 2018, 92, 2341-2344.	0.6	1
129	Formation of Acquired Grain-Growth Inhibitor in the Production of Anisotropic Electrical Steel. Steel in Translation, 2018, 48, 541-546.	0.3	1
130	Electrically Conducting Ceramics Based on Al–AlN–TiB2. High Temperature, 2018, 56, 527-531.	1.0	1
131	Estimating the Stability of the Structure of MAX Phases of Ti3AlC2–ÂÑBÑ Composition on the Basis of Quantum-Chemical Calculations. Russian Journal of Physical Chemistry A, 2019, 93, 1277-1280.	0.6	1
132	Ti–Zr Alloy by Magnesiothermic Reduction and Acid Leaching: Influence of Process Conditions. International Journal of Self-Propagating High-Temperature Synthesis, 2019, 28, 187-190.	0.5	1
133	Influence of the Preparation Method on Amorphous-Crystalline Transition in Fe84B16 Alloy. Technical Physics, 2019, 64, 1808-1813.	0.7	1
134	Direct Conversion of Chemical Energy into Electrical Energy in the Combustion of a Thin Three-Layer Charge. Combustion, Explosion and Shock Waves, 2019, 55, 678-685.	0.8	1
135	Composition and Crystalline Structure of Ternary Phases in the Ta–Ni–Al System. Russian Journal of Non-Ferrous Metals, 2020, 61, 303-308.	0.6	1
136	Mo5SiB2-Based Ceramics by Forced SHS Compaction and Hot Pressing of SHS-Produced Powders: Features of Phase-Formation Processes. International Journal of Self-Propagating High-Temperature Synthesis, 2020, 29, 143-149.	0.5	1
137	X-Ray Diffraction Study of a New Phase in the Ni–W–C System. Inorganic Materials, 2020, 56, 572-576.	0.8	1
138	SHS in the Cu–Se System. International Journal of Self-Propagating High-Temperature Synthesis, 2021, 30, 180-184.	0.5	1
139	Reduction of Mn, Cr, and V Precursors in a Wave of Flameless RDX Combustion. International Journal of Self-Propagating High-Temperature Synthesis, 2021, 30, 11-14.	0.5	1
140	Synthesis of Cu2 – nSe via Autowave Combustion of an Elemental Powder Mixture. Inorganic Materials, 2021, 57, 1124-1134.	0.8	1
141	Synthesis of Nanosized FeS, CoS and NiS Crystals in a Wave of Flameless RDX Combustion. International Journal of Self-Propagating High-Temperature Synthesis, 2021, 30, 220-224.	0.5	1
142	The Synthesis of Cast Materials Based on the MAX Phases in a Cr–Ti–Al–C System. Russian Journal of Non-Ferrous Metals, 2021, 62, 732-739.	0.6	1
143	Synthesis of Ta4HfC5 Ceramics with a Submicron Structure by Electro-Thermal Explosion under Pressure. Doklady Chemistry, 2021, 501, 259-263.	0.9	1
144	Deposition of composite metallic coating onto Al through mechanical impregnation followed by thermal treatment. International Journal of Self-Propagating High-Temperature Synthesis, 2010, 19, 178-185.	0.5	0

#	Article	IF	CITATIONS
145	Influence of the synthesis conditions of boron carbide on its structural parameters. Russian Journal of Non-Ferrous Metals, 2016, 57, 604-609.	0.6	0
146	X-Ray Diffraction Analysis of the Amorphous–Crystalline Phase Transition in Ni. Technical Physics, 2020, 65, 1652-1658.	0.7	0
147	Density Functional Theory Calculations of the Stability and Statistical Disorder in Crystals of the Kappa Phase of Me3Â+ÂxW10–ÂxC3Â+Ây (Me = Fe, Co, Ni). Russian Journal of Physical Chemistry A, 2020, 94, 1369-1374.	0.6	0
148	Ti–W Composite by Magnesiothermic SHS and Acid Leaching. International Journal of Self-Propagating High-Temperature Synthesis, 2020, 29, 36-41.	0.5	0
149	Formation of New Intermetallic Phases in the Ta–Ni–Al System. Inorganic Materials: Applied Research, 2020, 11, 271-276.	0.5	0
150	Combustion Modes of Mixtures of Nickel (II) Oxide with Titanium. Fizika Goreniya I Vzryva, 2021, 57, 69-72.	0.0	0
151	Subtle Details in Crystal Structure of SHS Products by DFT Calculations. International Journal of Self-Propagating High-Temperature Synthesis, 2021, 30, 15-21.	0.5	0
152	SHS in the Si–N–O System Containing Iron Salts. International Journal of Self-Propagating High-Temperature Synthesis, 2021, 30, 65-72.	0.5	0
153	Synthesis of W–Zr–Ti Alloy via Combustion in the WO3–ZrO2–TiO2–Mg System. Inorganic Materials, 2021, 57, 498-502.	0.8	0
154	Combustion Modes of Mixtures of Copper (II) Oxide with Aluminum and Titanium. Fizika Goreniya I Vzryva, 2021, 57, 67-73.	0.0	0
155	Combustion Modes of Mixtures of Copper (II) Oxide with Aluminum and Titanium. Combustion, Explosion and Shock Waves, 2021, 57, 570-575.	0.8	0
156	Time-Resolved X-Ray and Synchrotron-Ray Diffraction. , 2017, , 388-391.		0
157	Obtaining of Ti ₂ AlC and Ti ₃ AlC ₂ MAX phases by SHS with reduction stage. Izvestiya Vuzov Poroshkovaya Metallurgiya I Funktsional'nye Pokrytiya, 2020, , 36-40.	0.2	0
158	<i>In situ</i> study of heterogeneous media combustion processes by time Resolved XRD. Zavodskaya Laboratoriya Diagnostika Materialov, 2022, 88, 49-61.	0.5	0
159	Obtaining a High-Entropy Fe–Cr–Co–Ni–Ti Alloy by Mechanical Alloying and Electric Spark Plasma Sintering of a Powder Mixture. Russian Journal of Non-Ferrous Metals, 2021, 62, 716-722.	0.6	0
160	The Influence of Molybdenum and Titanium on Magnetic and Mechanical Properties of Fe–30Cr–16Co (Kh30K16) Powder Hard Magnetic Alloy. Steel in Translation, 2021, 51, 939-944.	0.3	0
161	Investigation of the Structure of Cyclodextrin Nitrates by the X-Ray Diffraction Method. Russian Journal of Applied Chemistry, 2022, 95, 32-36.	0.5	0